



Influence of GaCl carrier gas flow rate on properties of GaN films grown by hydride vapor-phase epitaxy

Yongliang Shao, Lei Zhang, Xiaopeng Hao*, Yongzhong Wu, Xiufang Chen, Shuang Qu, Xiangang Xu, Minhua Jiang

State Key Lab of Crystal Materials, Shandong University, Jinan, 250100, People's Republic of China

ARTICLE INFO

Article history:

Received 18 October 2010

Received in revised form 28 February 2011

Accepted 28 February 2011

Available online 8 March 2011

Keywords:

GaN

Hydride vapor-phase epitaxy

Semiconductors

ABSTRACT

The influence of GaCl carrier gas flow rate on GaN films grown by hydride vapor-phase epitaxy (HVPE) was investigated. The symmetric (0002) and asymmetric (10–12) ω scans were detected to estimate the quality of GaN films. Optical properties were studied by room temperature photoluminescence spectra. Raman spectroscopy was employed to analyze the residual stress in the samples. The surface morphology of the GaN films was investigated by atomic force microscopy (AFM). On the basis of process optimization the optimal GaCl carrier gas flow rate for growth of high quality GaN films in our system was obtained as 1.3 L/min.

© 2011 Elsevier B.V. All rights reserved.

1. Introduction

For the advanced performance as a semiconductor material of optical and electrical devices [1–3] and high-power high-frequency electronic devices [4], gallium nitride (GaN) has been studied by many groups in recent years. In order to get bulk crystal several methods, such as high-pressure solution (HPS) technique [5], ammonothermal growth technology [6], and Na-flux method [7] were employed to get GaN substrate with high crystalline quality. Stringent growth condition and anisotropy of growth rate in different directions were the disadvantage of these methods. The hydride vapor-phase epitaxy (HVPE) method was first used to grow GaN single-crystal about forty years ago [8]. It was demonstrated that the HVPE technique was a suitable and effective method for growth of bulk GaN crystals [9]. Crystals as thick as 5.8 mm can be grown at growth rates of 100–500 $\mu\text{m/h}$ along the crystallographic (0001) direction [10].

However, the lack of native substrates lead to the HVPE growth of GaN was mainly on foreign substrates [11,12]. There is high dislocation density in GaN because of the large lattice mismatch and thermal expansion coefficient mismatch between GaN and the substrate [13,14]. Some methods were used to enhance the crystalline quality of the heteroepitaxy GaN layer, such as epitaxial lateral overgrowth (ELOG) [15], overgrown on etch pits [16] and fabrication of nanostructure on substrate [17]. On the other hand, in

the HVPE system many conditions, such as growth temperature, pressure, the flow rate of various source and carrier gases, the distance between gases outlet and substrate and other, influence the growth process and the properties of GaN films. Complete HVPE experimental investigations were done to research the influence of growth temperature and the V/III ratio on the GaN grown with selective area substrates [18]. Influence of the partial pressure of GaCl_3 [19] and reactor pressure [20] in the growth process were researched to improve qualities of GaN layers grown by HVPE. The effects of shower head orientation and substrate position on the uniformity of GaN growth in a HVPE reactor were studied by computer simulation and geometric limitation of real experiments [21]. It is necessary to carefully investigate the growth condition of the initial stage of the HVPE process.

In this study the *impact* of one condition, GaCl carrier gas flow rate, on the properties of HVPE grown GaN films was investigated. In the present work the GaCl carrier gas flow rate was optimized to obtain heteroepitaxy GaN film with low dislocation density.

2. Experimental details

The growth process was carried out in a vertical HVPE system. The substrates for HVPE were 3–5 μm GaN layers fabricated by metal-organic chemical vapor deposition (MOCVD) on 2-in c-plane sapphire substrates. The substrate was faced down in the holder to the gases outlet and placed at the top of the reactor which was rotated at 20 rpm. Nitrogen (N_2) serving as the carrier gas blew in the whole reactor and delivered the source gases in the gases supply system fed from the bottom of the reactor. Ammonia (NH_3) was directly supplied with the N_2 carrier gas to the substrate as the nitrogen source. The GaCl was generated by passing a HCl/N_2 mixture through a tube into a boat with liquid gallium (*in accordance with the reaction* $2\text{HCl} + 2\text{Ga(liquid)} = 2\text{GaCl} + \text{H}_2$). The generated GaCl associated with N_2 was injected

* Corresponding author. Tel.: +86 53188366218; fax: +86 53188364864.
E-mail address: xphao@sdu.edu.cn (X. Hao).

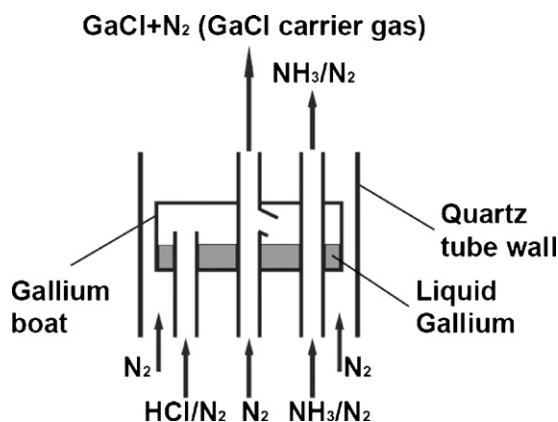


Fig. 1. Schematic diagram of the gases supply system and the gallium boat in the vertical-tube single-wafer reactor for GaN HVPE.

into the GaCl delivery tube and the mixed gas was sent to the substrate as the gallium source (see Fig. 1 for detail).

The HCl flow rate was set as 50 mL/min into the gallium boat which was heated to 820 °C. The NH_3 was at a V/III of 20 for growth of GaN films with a temperature of 1030 °C in the deposition zone. In the initial stage of the HVPE process the HCl flow rate was lower with a V/III of 80 to limit the growth rate which was beneficial to the crystal quality. A wide-range variation of GaCl carrier gas flow rates from 1.1 L/min to 2.3 L/min, 1.1 L/min, 1.3 L/min, 1.5 L/min, 1.8 L/min and 2.3 L/min, were employed in the HVPE growth. The experiments were done at atmospheric pressure. In this study all the other growth conditions were kept constant and the thickness of this series of HVPE GaN films was around 20 μm to exclude the influence of these conditions on the properties of the films.

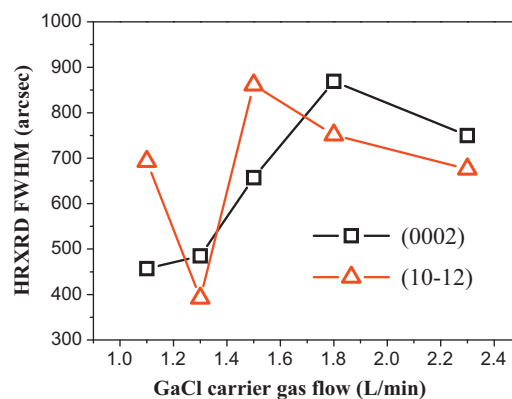


Fig. 2. The symmetric (0002) and asymmetric (10–12) ω scan FWHM of HVPE GaN films with different GaCl carrier gas flow rates.

The crystalline quality of the HVPE GaN films was confirmed by high-resolution X-ray diffraction (HR-XRD, PANalytical X'PERT PRO). The full width at half maximum (FWHM) of symmetric (0002) and asymmetric (10–12) ω scans were detected to compare the quality of GaN films grown by variation of GaCl carrier gas flow rates. Optical properties were determined by room temperature photoluminescence spectra which used a 325 nm He–Cd laser for excitation. Raman spectroscopy was employed to analyze the residual stress of the samples. The surface morphology of the grown GaN films was investigated by atomic force microscopy (AFM).

3. Results and discussion

The ω scans peak widths showed the same spread for the films exhibited a mosaic structure. The mosaic structure is described

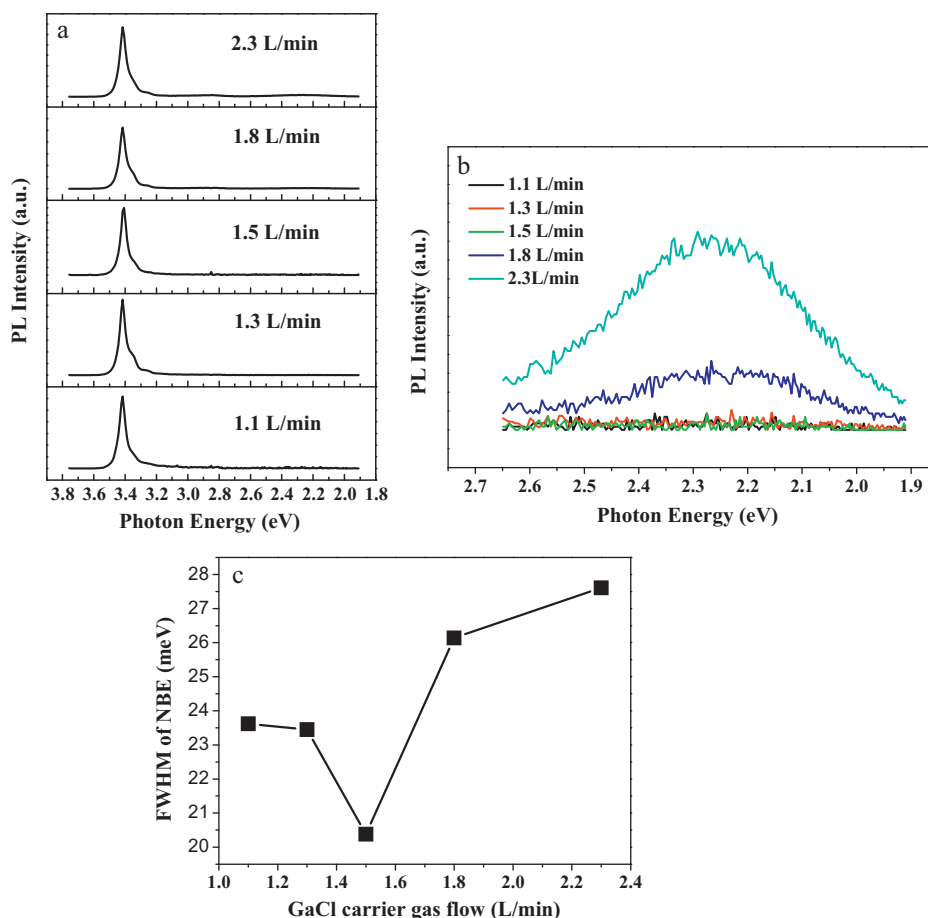


Fig. 3. Room temperature photoluminescence spectra of GaN films with different GaCl carrier gas flow rates. The PL spectra of different films (a), weak yellow luminescence (YL) peak at 2.26–2.29 eV (b) and the FWHM of NBE peak in different samples (c) are shown in this figure.

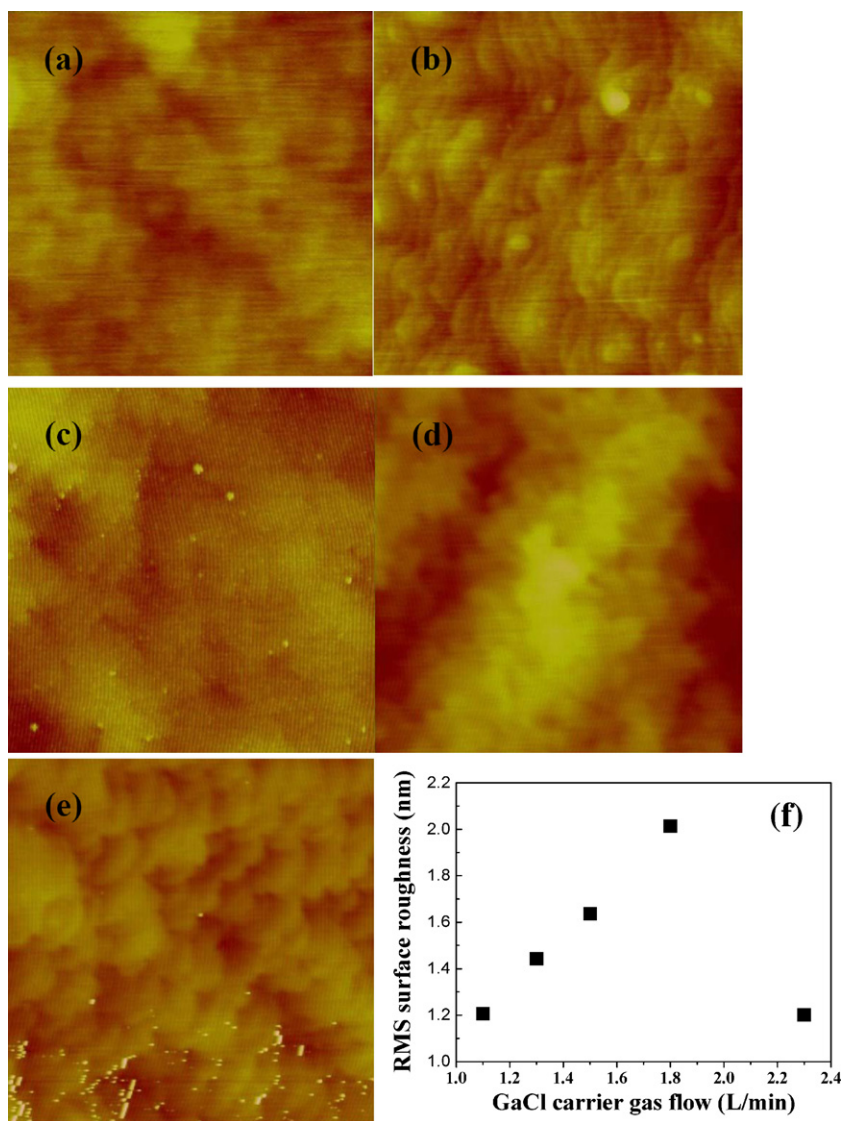


Fig. 4. Atomic force microscopy (AFM) images of the HVPE grown GaN films with GaCl carrier gas flow rate of 1.1 L/min (a), 1.3 L/min (b), 1.5 L/min (c), 1.8 L/min (d) and 2.3 L/min (e). The surface roughness (root mean square, RMS) of the HVPE grown GaN films with different GaCl carrier gas flow rates (f). The measured area was $5 \mu\text{m} \times 5 \mu\text{m}$.

by two crystallographic parameters: the range of tilt between the sub-grains and their range of twist. The sub-grain boundary is formed by three types of dislocations in GaN: a-type, c-type and a+c-type. Burgers vectors of the three types of dislocations were:

$$\vec{b}_a = 1/3 \langle 11\bar{2}0 \rangle \quad \vec{b}_c = \langle 0001 \rangle \quad \vec{b}_{a+c} = 1/3 \langle 11\bar{2}3 \rangle$$

The edge dislocation represented the pure a-type and a component of (a+c)-type dislocation, meanwhile, the screw dislocation referred to the pure c-type and c component of (a+c)-type dislocations. The FWHM of the symmetric ω scan of a GaN (0002) reflection is often applied to evaluate the tilt between sub-grains and the screw dislocation density. The twist of sub-grains, which is induced by edge dislocations, was difficult to obtain by direct measurement. The twist was obtained by the FWHM of asymmetric reflection combined with some mathematical methods, while the edge dislocation density was reflected by the FWHM of some asymmetric ω scans, in this study it was (10–12) ω scan [22,23]. Fig. 2 demonstrates the symmetric (0002) and asymmetric (10–12) ω scan XRD FWHM of HVPE GaN films with different GaCl carrier gas flow rates. For the (0002) reflection the FWHM was small

under the low GaCl carrier gas flow rates (1.1 and 1.3 L/min), while under high flow rates (1.8 and 2.3 L/min) the FWHM was large. But for the (10–12) reflection the lowest FWHM corresponded to 1.3 L/min. The FWHM of (0002) reflection is often applied to evaluate the screw dislocation density and the edge dislocation density is reflected by the FWHM of (10–12) reflection. The total dislocation density was the sum of screw and edge dislocation densities. So the 1.3 L/min GaCl carrier gas flow rate sample with low FWHM of both (0002) and (10–12) reflection was demonstrated to have high crystalline quality and low dislocation density. The low GaCl carrier gas flow rate increased the concentration of GaCl, so the growth rate was also increased. In the high GaCl carrier gas flow condition the concentration of GaCl was low, but the total flow rate was high for the high gas velocity caused by the high GaCl carrier gas flow rate, in this case, the growth rate was also high. The total GaCl gas is almost the same in different GaCl carrier gas flow rate condition. So the thickness of these GaN film is the same. However, from our results the low GaCl carrier gas flow rate was beneficial to enhance the HVPE GaN film quality. The best crystalline quality GaN film was demonstrated to be grown under the medium GaCl carrier gas flow rate condition, and in the present configuration the optimal value was around 1.3 L/min.

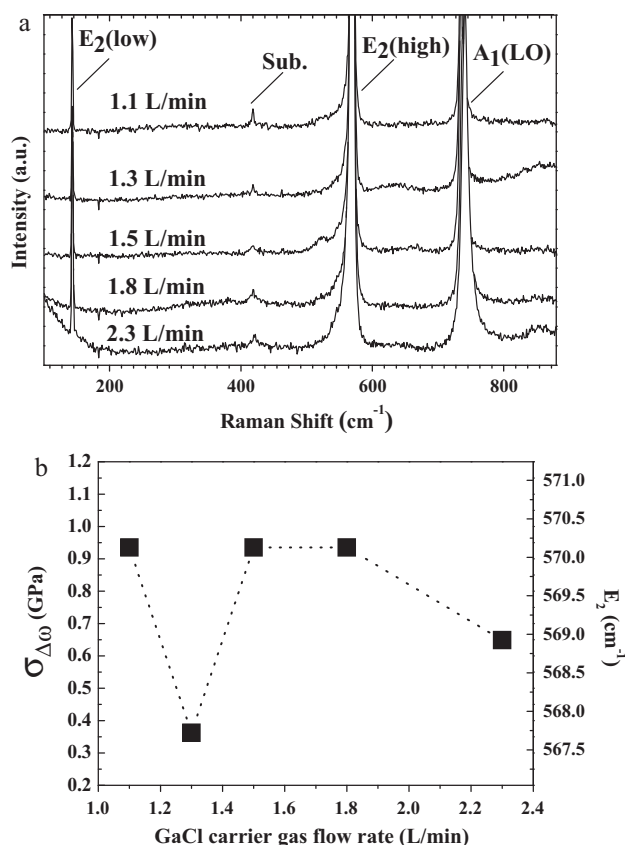


Fig. 5. Room temperature Raman spectra of HVPE GaN films grown at different GaCl carrier gas flow rate (a) as well as the residual stress and corresponding wave number of the high E_2 (high) mode (b).

The optical properties of HVPE GaN films obtained at different growth conditions were investigated by room temperature photoluminescence (PL) measurements (Fig. 3(a)). Strong near band-edge emission (NBE) with a peak position of 3.41–3.42 eV (363–364 nm) was observed from all samples (Fig. 3(b)). The FWHM of NBE peak was 20–30 meV in each sample. The film grown with 1.5 L/min GaCl carrier gas had the lowest FWHM of NBE; however in the films with higher and lower GaCl carrier gas flow rates the FWHM was high (Fig. 3(d)). This showed that the crystalline quality of 1.5 L/min film was better than the films with higher or lower GaCl carrier gas flow rates. The lowest NBE peak FWHM value was obtained under medium GaCl carrier gas flow rate. It was similar to the FWHM value of (10–12) asymmetric ω scan peak in HR-XRD results. The PL spectra of GaN films grown with high GaCl carrier gas flow rates had a very weak yellow luminescence (YL) peak at 2.26–2.29 eV (Fig. 3(c)). The yellow luminescence is caused by native defects such as vacancies, anti-sites and interstitials [24,25]. The very weak YL suggested that there is a low density of point defect in the grown samples. The results of room temperature PL spectra confirmed that the crystalline quality was higher in the GaN film under the medium GaCl carrier gas flow rate.

The surface morphology of the grown GaN films with different growth conditions was investigated by AFM. The measured sample area was 5 $\mu\text{m} \times 5 \mu\text{m}$. The surface morphology of all grown films showed a clear step flow growth mode (Fig. 4(a)–(e)). The surface roughness (root mean square, RMS) of the HVPE growth GaN films with different GaCl carrier gas flow rates is shown in Fig. 4(f). The surface RMS of these GaN films was 1.0–2.0 nm. This shows that all the films had a very flat growth surface.

Raman spectroscopy was employed to analyze the stress conditions of the samples under different growth conditions. The whole

spectrum measured shown in Fig. 5(a). The E_2 (high and low) and A_1 (LO) modes of GaN were detected in all GaN films. A weak peak of the sapphire substrate was observed at 418–419 cm⁻¹ in each sample. The E_2 (low) mode at 142.7 cm⁻¹ did not shift in the samples with different GaCl carrier gas flow conditions. It had been reported that a biaxial stress of one GPa would shift the E_2 (high) Raman mode by 4.2 cm⁻¹ and the wave number of stress-free standard GaN E_2 (high) Raman mode was at 566.2 cm⁻¹ [26]. The stress condition and corresponding wave number of the HVPE GaN films are shown in Fig. 5(b). The film grown with 1.3 L/min GaCl carrier gas flow rate was detected to have the lowest the residual compressive stress 0.36 GPa, which corresponded to the wave number of E_2 Raman mode at 567.7 cm⁻¹. The FWHM and line shape of A_1 (LO) mode peak related to the electron concentration and mobility of GaN according to the theory of phonon–plasmon coupled modes [27]. Detailed investigation of the A_1 (LO) behavior and the electrical properties on the HVPE grown GaN films will be reported in a future paper.

4. Conclusions

The properties of HVPE GaN films grown under different GaCl carrier gas flow conditions were studied to obtain optimal condition for high crystalline quality GaN film. The 1.3 L/min GaCl carrier gas flow rate sample with low FWHM of both (0002) and (10–12) reflection was demonstrated to have high crystalline quality and low dislocation density. Room temperature photoluminescence results showed a strong band-edge emission (NBE) peak with a FWHM of 20–30 meV which was detected in each sample. GaN films grown by high GaCl carrier gas flow rate had a very weak yellow luminescence (YL) peak at 2.26–2.29 eV. The surface morphology of all films showed a clear step flow growth model in AFM images. The HVPE GaN films grown with 1.3 L/min GaCl carrier gas flow rate were found to have the lowest the residual compressive stress 0.36 GPa, which corresponded to the wave number of E_2 Raman mode at 567.7 cm⁻¹. On the basis of the characterization results obtained, the optimal GaCl carrier gas flow rate for growth of high crystalline quality films was determined as 1.3 L/min.

Acknowledgement

This work was supported by NSFC (Contract No. 50823009, 51021062), National Basic Research Program of China (2009CB930503), the Key Project of Chinese Ministry of Education (No. 109096), the Scientific Development Planning of Shandong Province (2010GGX10340). Thanks to Dr. Edward C. Mignot, Shandong University, for linguistic advice.

References

- [1] S. Nakamura, T. Mukai, M. Senoh, Appl. Phys. Lett. 64 (1994) 1687–1689.
- [2] D. Ehrentraut, Z. Sitar, MRS Bull. 34 (2009) 259–265.
- [3] D.G. Zhao, D.S. Jiang, J.J. Zhu, H. Wang, Z.S. Liu, S.M. Zhang, Y.T. Wang, Q.J. Jia, H. Yang, J. Alloys Compd. 489 (2010) 461–464.
- [4] M. Bawedin, M.J. Uren, F. Udrea, Solid-State Electron. 54 (2010) 616–620.
- [5] I. Grzegory, M. Boćkowska, P. Strąka, S. Krukowska, S. Porowska, J. Cryst. Growth 312 (2010) 2593–2598.
- [6] Y. Kagamitani, T. Kuribayashi, K. Hazu, J. Cryst. Growth 312 (2010) 3384–3387.
- [7] K. Fujito, S. Kubo, H. Nagaoka, et al., J. Cryst. Growth 310 (2008) 3946–3949.
- [8] H.P. Maruska, J.J. Tietjen, Appl. Phys. Lett. 15 (1969) 327–329.
- [9] H. Ashrafi, R. Kudrawiec, J.L. Weyher, et al., J. Cryst. Growth 312 (2010) 2398–2403.
- [10] F. Kawamura, M. Morishita, M. Tanpo, et al., J. Cryst. Growth 311 (2009) 3011–3014.
- [11] S. Qu, S. Li, Y. Peng, X. Zhu, X. Hu, C. Wang, X. Chen, Y. Gao, X. Xu, J. Alloys Compd. 502 (2010) 417–422.
- [12] J. Zou, W.D. Xiang, J. Alloys Compd. 484 (2009) 622–625.
- [13] D. Kapolenek, X.H. Wu, B. Heying, S. Keller, B. Keller, U.K. Mishra, S.P. Denbaars, J.S. Speck, Appl. Phys. Lett. 67 (1995) 1541–1543.

- [14] W. Qian, M. Skowronski, M. Degraef, K. Doverspike, L.B. Rowland, D.K. Gaskill, Appl. Phys. Lett. 66 (1995) 1252–1254.
- [15] H.H. Huang, C.L. Chao, T.W. Chi, Y.L. Chang, P.C. Liu, L.W. Tu, J.D. Tsay, H.C. Kuo, S.J. Cheng, W.I. Lee, J. Cryst. Growth 311 (2009) 3029–3032.
- [16] W. Zhang, Q.Y. Hao, C.C. Liu, Y.C. Feng, J. Alloys Compd. 456 (2008) 368–371.
- [17] C.L. Chao, C.H. Chiu, Y.J. Lee, H.C. Kuo, P.C. Liu, J.D. Tsay, S.J. Cheng, Appl. Phys. Lett. 95 (2009) 051905–051907.
- [18] O. Chelda-Gourmala, A. Trassoudaine, et al., J. Cryst. Growth 312 (2010) 1899–1907.
- [19] E. Aujol, A. Trassoudaine, D. Castelluci, R. Cadoret, Mater. Sci. Eng. B: Solid 82 (2001) 65–67.
- [20] X.C. Cao, D.L. Xu, H.M. Guo, et al., Thin Solid Films 517 (2009) 2088–2091.
- [21] W.C. Lan, C.D. Tsai, C.W. Lan, J. Taiwan Inst. Chem. Eng. 40 (2009) 475–478.
- [22] P. Gay, P.B. Hirsch, A. Kelly, Acta Metall. Mater. 1 (1953) 315–319.
- [23] V. Srikant, J.S. Speck, D.R. Clarke, J. Appl. Phys. 82 (1997) 4286–4295.
- [24] J.L. Lyons, A. Janotti, C.G. Van de Walle, Appl. Phys. Lett. 97 (2010) 152108.
- [25] F.J. Xu, B. Shen, L. Lu, et al., J. Appl. Phys. 107 (2010) 023528.
- [26] C. Kisielowski, S. Ruvimov, T. Suski, Phys. Rev. B 54 (1996) 17745–17753.
- [27] T. Kozawa, T. Kachi, H. Kano, Y. Taga, M. Hashimoto, N. Koide, K. Manabe, J. Appl. Phys. 75 (1994) 1098–1101.